Title

Fine processes of Nestin-GFP–positive radial glia-like stem cells in the adult dentate gyrus ensheathe local synapses and vasculature

Journal

Proceedings of the National Academy of Sciences of the United States of America, 113(18)

ISSN

0027-8424

Authors

Moss, Jonathan
Gebara, Elias
Bushong, Eric A
et al.

Publication Date

2016-05-03

DOI

10.1073/pnas.1514652113

Peer reviewed

Fine processes of Nestin-GFP–positive radial glia-like stem cells in the adult dentate gyrus ensheathe local synapses and vasculature

Jonathan Moss[a], Elias Gebara[a], Eric A. Bushong[b], Irene Sánchez-Pascual[a], Ruadhan O'Laoi[a], Imane El M'Ghari[a], Jacqueline Kocher-Braissant[a], Mark H. Ellisman[b], and Nicolas Toni[a,1]

[a]Department of Fundamental Neurosciences, University of Lausanne, 1005 Lausanne, Switzerland; and [b]National Center for Microscopy and Imaging Research, University of California, San Diego, La Jolla, CA 92093

Edited by Heather A. Cameron, National Institute of Mental Health/National Institutes of Health, Bethesda, MD, and accepted by the Editorial Board March 16, 2016 (received for review July 29, 2015)

Adult hippocampal neurogenesis relies on the activation of neural stem cells in the dentate gyrus, their division, and differentiation of their progeny into mature granule neurons. The complex morphology of radial glia-like (RGL) stem cells suggests that these cells establish numerous contacts with the cellular components of the neurogenic niche that may play a crucial role in the regulation of RGL stem cell activity. However, the morphology of RGL stem cells remains poorly described. Here, we used light microscopy and electron microscopy to examine Nestin-GFP transgenic mice and provide a detailed ultrastructural reconstruction analysis of Nestin-GFP–positive RGL cells of the dentate gyrus. We show that their primary processes follow a tortuous path from the subgranular zone through the granule cell layer and ensheathe local synapses and vasculature in the inner molecular layer. They share the ensheathing of synapses and vasculature with astrocytic processes and adhere to the adjacent processes of astrocytes. This extensive interaction of processes with their local environment could allow them to be uniquely receptive to signals from local neurons, glia, and vasculature, which may regulate their fate.

adult neurogenesis | adult neural stem cell | neurogenic niche | electron microscopy | hippocampus

Neurogenesis in the adult mouse brain primarily occurs within discrete niches, the subventricular zone (SVZ), and the subgranular zone (SGZ) of the dentate gyrus, supplying new neurons to the olfactory bulb and the dentate gyrus, respectively (1–3). Neural stem cells of these niches can be activated to divide and generate other stem cells, astrocytes, or new neurons (4, 5). Newborn neurons of the dentate gyrus have the capacity to integrate into the existing hippocampal circuitry (6–8), influencing processes such as learning and memory (9–11) as well as stress and depression (12).

Radial glia-like (RGL) neural stem cells of the SVZ, which supply the olfactory bulb with newborn neurons and astrocytes, express astrocytic markers and form elegant pinwheel structures (13–16). RGL neural stem cells of the adult dentate gyrus also express astrocytic markers, but comprise a heterogeneous population based on the molecular markers they express, the morphologies they exhibit (17–22), and their fate (23–28). Nestin-GFP–positive RGL stem cells account for more than 70% of RGL stem cells in the SGZ of the dentate gyrus (24), but it was recently found that not all Nestin-GFP–positive cells with RGL morphology have stem cell properties (29): type β cells, which arborize in the granule cell layer (GCL) but do not reach the molecular layer (ML) of the dentate gyrus, account for 26% of Nestin-GFP–positive RGL stem cells. They express stem cell (Sox1, Sox2, Prominin 1, GFAP, and Nestin) and astrocytic [GFAP, glial glutamate tranporter 1 (GLT1), and S100β] markers but do not proliferate. In contrast, type α cells, which extend across the GCL and arborize in the inner ML, account for 74% of Nestin-GFP–positive RGL cells. They express stem cell markers such as Sox1, Sox2, Prominin 1, GFAP, and Nestin, but neither S100β nor GLT1. Fate clonal analysis shows that these cells are able to proliferate and generate more type α cells, type 2 neuronal progenitors, astrocytes, and nonproliferative type β cells. In this study, we therefore focused on type α Nestin-GFP–positive RGL stem cells (hereafter referred to as NGPα RGL stem cells), which form dense arborizations of fine processes in the inner ML.

So why do these NGPα RGL stem cells have such a complex radial morphology? Embryonic cortical stem cells have smooth spheroid cell bodies that extend long smooth processes, which enable newly formed neurons to migrate into the cortical plate (30). In the adult dentate gyrus, however, the observation of individual clones suggest that adult-born neurons do not migrate alongside the radial process of their mother cells, but instead migrate tangentially away from it, before integrating into the GCL (24, 31). We therefore believe that the reasons for their complex radial morphologies lie in the regulatory mechanisms of the neurogenic niche. Adult neurogenesis is tightly regulated by the neurogenic niche, primarily restricting it to the SGZ and the SVZ, despite the neurogenic potential of progenitors that can be found throughout the central nervous system (32–34). The niche is vital for adult neurogenesis, and we suspect the elaborate morphology of RGL stem cells is key for their regulation by elements of the neurogenic niche (29, 35).

Significance

A population of adult neural stem cells supplies the dentate gyrus with new neurons that play a role in mechanisms of learning and memory. Radial glia-like stem cells have a unique morphology, including a dense arbor of fine processes that infiltrate the neurogenic niche. Here, we provide what is, to our knowledge, the first detailed ultrastructural description of these processes, and we reveal that these cells establish a variety of contacts with local blood vessels, synapses, and astrocytes. Given that signals derived from neurons, astrocytes, and blood vessels regulate the process of adult neurogenesis, the identification of these contacts provides a structural framework for elucidating the mechanisms by which this regulation occurs. These results contribute to a greater understanding of the adult hippocampal neurogenic niche.

Author contributions: J.M. and N.T. designed research; J.M., E.G., E.A.B., I.S.-P., R.O., I.E.M., and J.K.-B. performed research; E.A.B. and M.H.E. contributed new reagents/analytic tools; J.M. analyzed data; and J.M. and N.T. wrote the paper.

The authors declare no conflict of interest.

This article is a PNAS Direct Submission. H.A.C. is a guest editor invited by the Editorial Board.

[1]To whom correspondence should be addressed. Email: nicolas.toni@unil.ch.

This article contains supporting information online at www.pnas.org/lookup/suppl/doi:10.1073/pnas.1514652113/-/DCSupplemental.

We use a variety of light microscopy (LM) and EM techniques to probe the fine anatomical structure of NGPα RGL stem cells and their contacts with the neurogenic niche. We describe in detail the relationship of NGPα RGL stem cell processes with the local vasculature, glia, and neurons in an effort to better understand the role their structure could play in the context of adult neurogenesis.

Results

NGPα RGL Stem Cell Processes Reflect Their Environment. To examine the morphology of the NGPα RGL stem cells in the dentate gyrus, we used Nestin-GFP transgenic mice (36, 37). Immunohistochemistry allowed us to render the GFP-positive cells electron-dense with a 3,3′-diaminobenzidine (DAB)-peroxidase reaction for visualization at LM and EM levels (*Materials and Methods*). Strong labeling of cells in the dentate gyrus was evident at the LM level (Fig. 1*A*), with dark bands of NGP RGL stem cell bodies and type 2 precursors delineating the SGZ between the hilus and GCL. Single NGPα RGL stem cells ($n = 7$; *Materials and Methods*) were selected from the population for examination when the majority of their processes were contained within one 50-μm section (Fig. 1*B*). First, this allowed us to confirm the identity of the given NGPα RGL stem cell, as Nestin can label other cell types in the dentate gyrus (36), but none with the same distinctive morphology of NGPα RGL stem cells. Second, the systematic tracing in 3D of all processes in the ML until their point of origin in the main process of the identified NGPα RGL stem cell enabled us to confirm their identity. Third, restricting our analyses to cells contained within one section maximized the proportion of each cell that could be examined.

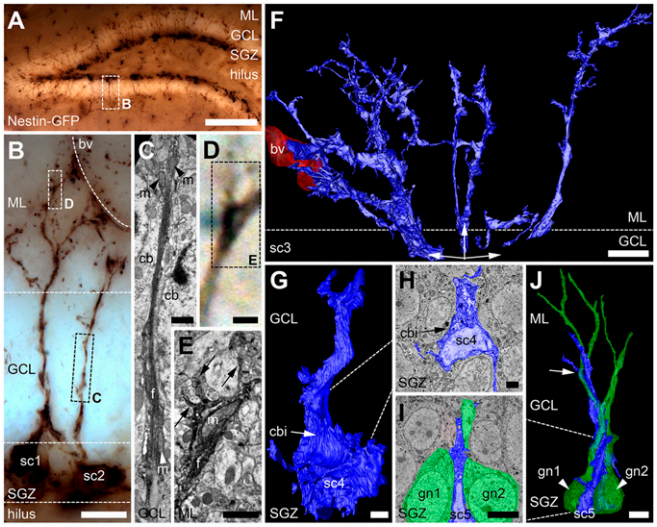

Fig. 1. RGL stem cell processes reflect their environment. (*A*) Dentate gyrus, immunoperoxidase-labeled for GFP, shows dark RGL stem cells and type 2 progenitor cells in the SGZ. (*B*) Two NGPα RGL stem cells (sc1 and sc2) from *A* extend their primary processes across the GCL that branch at the border of the ML, with some branches approaching a blood vessel (bv). (*C*) Detail from *B*: EM frame shows primary process of RGL stem cell (sc2) replete with filamentous fibers (f), constricted by two cell bodies (cb) in the GCL. Before and after the constriction, mitochondria (m) can be seen inside the process. (*D* and *E*) Detail from *B*: correlative LM (*D*) and EM (*E*) images of a mitochondria-containing portion of the process (m) where intracellular fibers (f) terminate, and finer processes (arrows) extend into the ML. (*F*) Processes of a single RGL stem cell (sc3) reconstructed from 178 SBF-SEM images. Three processes extend toward a local blood vessel (bv, red; Movie S1). (*G* and *H*) Three-dimensional reconstruction (*G*) from SBF-SEM images (*H*) of an RGL stem cell (sc4, blue) with neighboring cell body indentations (cbi; Movie S2). (*I* and *J*) Three-dimensional reconstruction of an RGL stem cell (sc5, blue) and its primary process (arrow) alongside two granule neurons (gn1 and gn2, green; Movie S3). (Scale bars: *A*, 100 μm; *B*, 10 μm; *C–E*, 1 μm; *F*, *I*, and *J*, 5 μm; *G* and *H*, 2 μm.)

Initial analyses showed that the primary processes of NGPα RGL stem cells, that extended across the GCL, were a key feature. Under the light microscope, they ostensibly appeared thicker and straighter than the subsequent secondary and tertiary processes in the ML (Fig. 1*B*). However, by using serial section transmission EM (TEM) and 3D reconstructions, primary processes were seen to twist and turn and expand and contract to infiltrate between the cell bodies of granule neurons (Fig. 1*C*). This is in contrast to the thinner and straighter processes of type 3, doublecortin-positive cells that also extend across the GCL (38). In the thinnest regions, only filamentous fibers occupied the process. Thicker, mitochondria-containing portions of the primary process gave rise to secondary branches (see also ref. 20). When the primary process had breached the border between the GCL and ML, extensive branching created large arbors of fine processes. Larger branches gravitated toward local blood vessels (Fig. 1*B*), whereas finer processes infiltrated the local neuronal and glial architecture (Fig. 1 *D* and *E*). The arborization of fine processes was generally confined to the inner third of the ML, but, occasionally, long fine threads reached as far as the outer third of the ML.

To complement our TEM observations, we used serial block-face scanning EM (SBF-SEM) (39) to image and reconstruct in 3D the fine ML processes of a single NGPα RGL stem cell (Fig. 1*F* and Movie S1). This reconstruction, and the individual frames from which it was created, revealed a great many features that could have been missed with the smaller sample sizes of TEM (Fig. S1*A*). The most obvious of these features was that larger ML secondary processes covered the surfaces of mature granule cell dendrites as they grew radially. This created the effect of processes forming a series of tunnels through which the mature dendrites extended (Fig. S1 *B–D*). Likewise, processes at the GCL–ML border displayed large concave surfaces, where they were positioned around the side of granule cell bodies (Fig. S1*E*). In addition to this main observation, several other features were worth noting: (*i*) a thick secondary process, on the edge of the ML, expanded to completely enclose a dendritic spine and the axons apposing the head of the spine (Fig. S1 *E* and *F*); (*ii*) a large process, extending toward a blood vessel, thinned into a sheet-like process between the edge of a cell body and large dendritic shaft (Fig. S1 *G* and *H*); and (*iii*) a thin sheet-like process extended tangentially, from a small radial process, and wrapped a number of axons along its path (Fig. S1 *I* and *J*).

The cell bodies of NGPα RGL stem cells took on three main morphologies: (*i*) they appeared pyramidal in nature, when their upper extreme was confined between the bases of granule neuron cell bodies of the GCL, and their lower extremes extended with greater freedom within the SGZ (Fig. 1 *G* and *H* and Movie S2); (*ii*) when their cell body sat entirely below the GCL, it appeared spheroid in shape (Fig. 1*B*, *sc2*); and (*iii*) on other occasions, the cell body was effectively sandwiched between two granule neuron cell bodies, and took on an hourglass-like conformation (Fig. 1 *I* and *J* and Movie S3). For all three morphologies, the surfaces of the stem cell body appeared concave, where granule neuron cell bodies impinged upon it, with ridges in between. Their nuclei almost completely filled the cytoplasm of the cell body and, as a result, took on the shape of the cell bodies themselves. Basal processes extended from the corners of their cell body, along the axis of the SGZ and into the hilus, and the primary process of the stem cell followed the dendrites of mature granule cells as they traversed the GCL.

Large NGPα RGL Stem Cell Processes Wrap Local Blood Vessels. One of most striking features of NGPα RGL stem cell morphology at LM and EM levels is their affinity to extend large processes toward local blood vessels (17, 19, 20, 29, 36), as visualized with

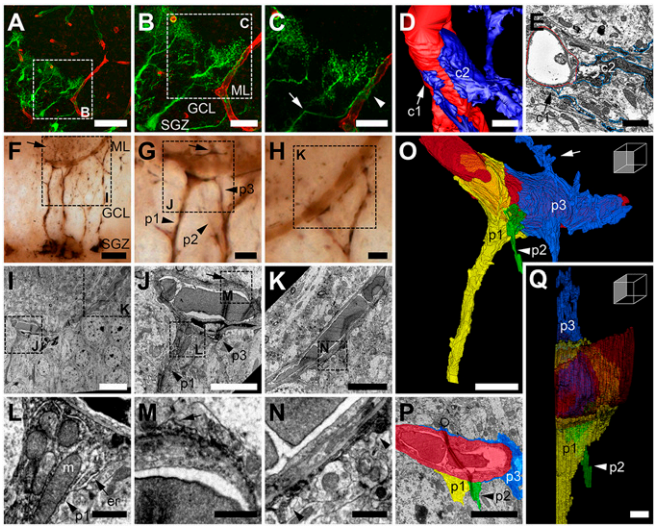

Fig. 2. RGL stem cell processes wrap blood vessels. (*A*–*C*) Confocal microscopy images of an NGPα RGL stem cell (green) branching toward (arrow) and contacting (arrowhead) a blood vessel (red; sulforhodamine 101). (*D*) Processes from a NGPα RGL stem cell (blue) making endfeet-like contacts (c1 and c2) with a local blood vessel (red); image 3D-reconstructed from SBF-SEM frames (*E*). (*F*) LM image of several NGPα, peroxidase-labeled RGL stem cells extending processes toward a blood vessel. (*G* and *H*) Higher-magnification images of *F*, with processes 3D-reconstructed in *O*–*Q* identified (p1–p3). (*I*–*K*) Correlative EM images of the interaction seen at the LM level in *F*–*H*. Arrows in *F*, *G*, *J*, *M*, and *O* show where the wrapping process (p3) extends beyond the blood vessel. (*L*) Detail from *J* shows mitochondria (m) and endoplasmic reticulum (er) clustered where process p1 spreads to ensheathe the blood vessel. (*M* and *N*) Detail from *J* and *K* showing thin wrapping of the blood vessel. (*O*–*Q*) Three-dimensional reconstruction (*O* and *Q*) and single EM frame (*P*) of the three processes (p1–p3) from two NGPα RGL stem cells (cell 1, p1, yellow; cell 2, p2, green; and cell 2, p3, blue) contacting/wrapping the blood vessel (red), originally seen in *F*, *G*, *I*, and *J* (Movie S4). (Scale bars: *A*, 50 μm; *B* and *F*, 20 μm; *C* and *I*, 10 μm; *D* and *E*, 2 μm; *G* and *H*, 5 μm; *J*, *K*, *O*, and *P*, 5 μm; *L*–*N* and *Q*, 1 μm.)

confocal microscopy (Fig. 2 *A*–*C*). For EM analyses of this interaction, we used DAB-peroxidase labeling of GFP in the Nestin-GFP mouse. Three-dimensional reconstruction of a single NGPα RGL stem cell (Fig. 2*D*) from serial SBF-SEM images (Fig. 2*E*) demonstrated its propensity to extend several large processes to contact the surface of a local blood vessel. These interactions ranged from small contacts (1–2 μm across), akin to astrocytic endfeet, up to larger sheet-like contacts that spread extensively (over 10 μm) across the surface of the blood vessel. NGPα RGL stem cells examined in a previous study were all shown to possess at least one interaction with a blood vessel (29). In the present study, we found that, if an ML blood vessel was situated only on one side of where the process emerged from the GCL, thick processes would polarize toward the blood vessel (Fig. 1 *B* and *F*). Conversely, stem cell process arbors would remain relatively symmetrical if blood vessels were (*i*) situated further from the emergence point, (*ii*) on both sides of the emergence point (at equal distances), or (*iii*) growing along the GCL–ML border (Fig. 2*F*).

To analyze how multiple NGPα RGL stem cell processes wrapped an individual blood vessel at the GCL–ML border, a region of tissue was selected for correlative LM/EM (Fig. 2*F*). This region contained an area where multiple processes from multiple NGPα RGL stem cells converged onto the blood vessel (Fig. 2*G*) and also an area where fewer processes approached the blood vessel (Fig. 2*H*). For larger processes, contacting or wrapping of the blood vessel did not represent the termination of their radial path, as finer processes branched beyond the blood vessel (Fig. 2 *F*, *G*, *J*, *M*, and *O*). EM analysis (i.e., TEM) of how the NGPα RGL stem cell process contacted the blood vessel revealed several key aspects of the interaction (Fig. 2 *I*–*N*). At the point where the primary process first met the blood vessel, the process expanded as it spread across the vessel surface (Fig. 2*J*), and within the expanded process sat a host of mitochondria and strings of endoplasmic reticulum (Fig. 2*L*). As processes wrapped the blood vessels, they thinned dramatically (Fig. 2 *J*, *K*, *M*, and *N*), but their coverage of the blood vessels was extensive.

Tracing these thin processes in serial EM sections and reconstructing them in 3D (Fig. 2 *O*–*Q*) revealed that they represented thin sheets of process that covered large areas of the blood vessel surface. Very few mitochondria were present within these thin sheets, perhaps explaining why so many were clustered at its point of origin (Fig. 2*L*), given the likely energy demands of possessing such an expansive morphology. The 3D reconstruction (Fig. 2 *O*–*Q* and Movie S4) showed three NGPα RGL stem cell processes, from two different cells, converging upon the same blood vessel and apposing each other along its surface. Of these three, two (Fig. 2 *O*–*Q*, p1 yellow and p3 blue) were larger processes that formed thin sheets and extended into fine processes beyond the blood vessel. The other (Fig. 2 *O*–*Q*, p2 green) branched from the same primary process as one of the larger processes (Fig. 2 *O*–*Q*, p3 blue) but had a much more restricted interaction with the blood vessel.

NGPα RGL Stem Cells and Astrocytes Share Blood Vessel Coverage. Processes of NGPα RGL stem cells covered much of the blood vessel surface, especially when the vessel was situated adjacent to the primary process emerging from the GCL. However, even in these regions, not all of the blood vessel was covered by the processes of a given labeled stem cell. The unlabeled processes covering the remainder of the blood vessel surface were similar in appearance to labeled processes, suggestive of a glial origin. Indeed, when they were examined in serial sections and 3D and traced to their larger processes and cell bodies in the ML, their morphologies were unmistakably those of astrocytes, characterized by bundles of filaments, granules of glycogen, a relatively pale cytoplasm, and condensations of chromatin inside the nuclear envelope (Fig. 3*A*) (40).

Astrocytes of the ML of the dentate gyrus and other regions of the hippocampus can position their cell bodies directly adjacent to blood vessels, completely enclosing large sections of a vessel (41, 42). However, in the vicinity of an NGPα RGL stem cell process emerging from the GCL, astrocytic coverage of the blood vessel was not always complete; the two types of process shared coverage of the blood vessel (Fig. 3*A*). The thickness of the stem cell process would expand and match the thickness of the astrocytic process, and form adhesion points where they met on the surface of the blood vessel, in direct contact with the basal lamina.

When blood vessels were more distant from the astrocyte cell body, multiple astrocytic processes shared the surface of the blood vessel, along with multiple NGPα RGL stem cell processes (Fig. 3 *B*–*D*). Examining the surface of a GCL–ML border blood vessel in cross-section, through 92 serial EM sections (each 70 nm thick), showed coverage by five stem cell processes and four astrocytic processes (Fig. 3 *E*–*R* and Movie S5). Along this section of blood vessel, the proportion of its surface covered by the stem cell process varied from approximately 50% to nearly 100% in individual sections (Fig. 3 *F*–*K*). Similar to the wrapping of the blood vessel by stem cell processes, astrocytic processes sometimes contacted the vessel with small endfeet (Fig. 3 *J* and *L*–*R*, astro2), and, on other occasions, contacts were made by large sheet-like processes (Fig. 3 *I* and *L*–*R*, astro3).

Fine Processes of NGPα RGL Stem Cells Approach Local Synapses. The primary or secondary processes of NGPα RGL stem cells split into a multitude of fine processes at the GCL–ML border, creating

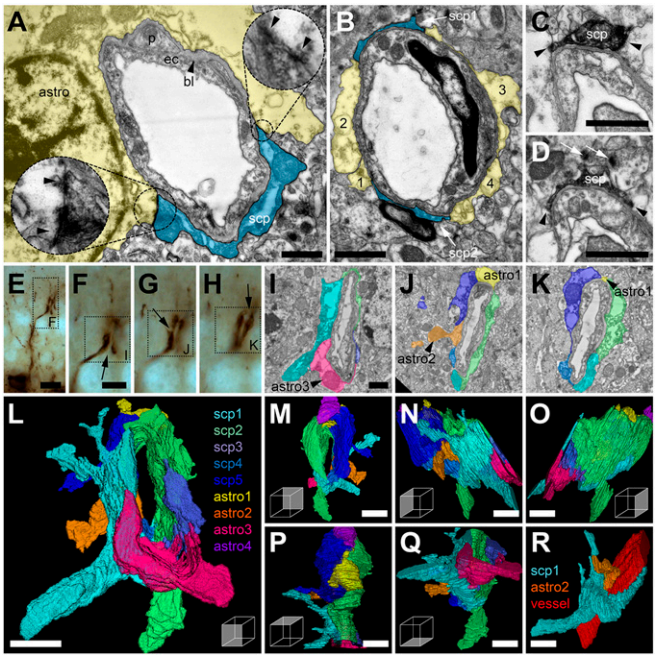

Fig. 3. RGL stem cell and astrocytic processes share coverage of blood vessels. (*A*) EM of an NGPα RGL stem cell process (scp, blue) wrapping a blood vessel in the inner ML that is also covered by astrocytic processes (astro, yellow): endothelial cell (ec), pericyte (p), basal lamina (bl). (*Insets*) Adhesion point densities (arrowheads) between astrocyte and stem cell processes. (*B*) Astrocytic processes (*1–4*, yellow) cover the blood vessel surface alongside NGPα RGL stem cell processes (scp1 and scp2, blue). (*C* and *D*) Serial sections of *B* show adhesion points (arrowheads) between NGPα RGL stem cell (scp) and astrocyte processes (*C*), and the same stem cell process extending toward synapses (arrows, *D*). (*E–H*) LM of an NGPα RGL stem cell wrapping a blood vessel at the GCL–ML border, seen at higher magnification in three different focal planes (*F–H*). Arrows in *F–H* point to the gaps in the stem cell process wrapping that correspond to the astrocytes seen in the EM frames (*I–K*). Processes are colored according to the key in *L*. (*L–R*) Three-dimensional reconstruction and alternate views of the five NGPα RGL stem cell processes and four astrocytic processes (Movie S5) that wrap the blood vessel depicted in *E–K*. (*R*) One astrocyte and one NGPα RGL stem cell process are shown with the blood vessel. (Scale bars: *A–D* and *I–K*, 1 μm; *E*, 10 μm; *F–H*, 5 μm; *L–R*, 2 μm.)

a dense arbor of intertwining fibers (Fig. 4 *A* and *B*) (17, 19, 20). Branching occurred abruptly, with stubs of large primary or secondary processes sprouting many fine processes. The fine processes took the form of long-reaching tendrils studded with varicosities (Fig. 4*B*). The varicosities were similar to those seen in the finest of thin neuronal dendrites, when the dendrite swells to incorporate small mitochondria at regular points along its length. When NGPα RGL stem cell process varicosities were analyzed at the EM level (Fig. 4 *C–E*), the vast majority contained a single mitochondrion, but notably the mitochondrion did not define the size of the varicosity. On average, the mitochondrion would only occupy 28% of the whole varicosity (±3%, SEM; $n = 10$; Fig. 4*F*). This raises the possibility that other intracellular machinery is occupying the remaining 72% of the varicosity, perhaps suggesting that varicosities represent a site for intercellular signaling.

To investigate this possibility further, we labeled NGPα RGL stem cells with immunogold particles. This allowed a greater visualization of the intracellular constituents than was possible with the DAB-peroxidase method, which fills the intracellular space with a dark diffuse reaction product. No evidence was found for any degree of synaptic contact with the immunogold-labeled varicosities, or any other part of the immunogold-labeled NGPα RGL stem cells. This does not rule out the presence of nonsynaptic receptors and associated intracellular machinery. Additionally, when a string of varicosities was viewed at the EM level, traced, and reconstructed in 3D (Fig. 4 *G–I* and Movie S6), three observations were made: (*i*) the radial process apposed and followed the primary and secondary dendrite of a mature granule neuron, as reported previously (38); (*ii*) fine processes extended from the varicosities to wrap local axons (Fig. 4 *J* and *K*); and (*iii*) some of these fine processes approached the synaptic cleft of local asymmetrical synapses, some of which were made with the spines of the granule cell dendrite the stem cell process was following (Fig. 4 *L* and *M*). It is possible that a common neuron-stem cell signaling mechanism underlies these three associations.

Fine Processes Ensheathe Asymmetrical Synapses. To more closely examine the association of fine NGPα RGL stem cell processes with local ML asymmetrical synapses, four NGPα RGL stem cells were selected from the dentate gyri of three Nestin-GFP DAB-peroxidase–labeled animals and then sectioned for EM analysis. It was possible to distinguish two types of interactions made by the varicosities with local asymmetrical synapses, although, in essence, they probably represent the extremes of a continuum. First, the varicosity itself wrapped its surfaces around

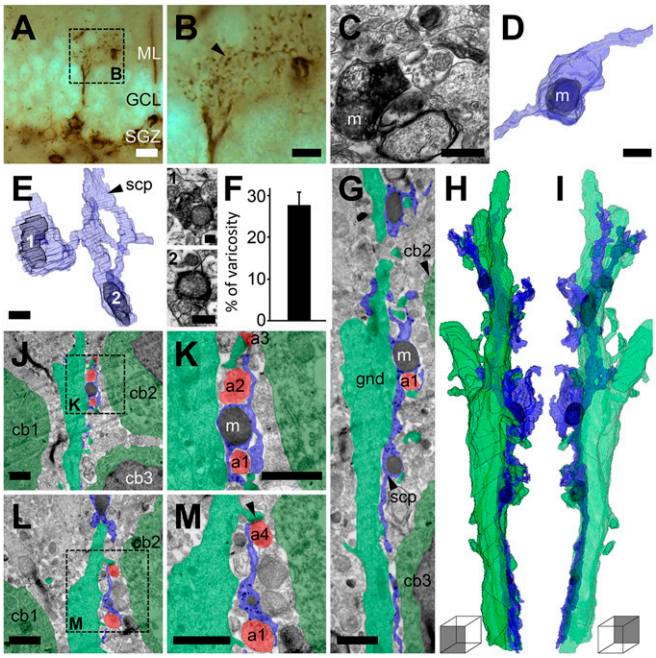

Fig. 4. Fine processes extend from varicosities of RGL stem cell processes to approach local synapses. (*A*) An NGPα DAB-peroxidase–labeled RGL stem cell selected for analysis of its fine process arbor at the GCL–ML border. (*B*) Higher-magnification view of the fine processes branching from primary and secondary processes. A fine process that resembles a long beaded string, because of the presence of varicose regions, extends toward a blood vessel (right). One mitochondrion-containing (m) varicosity from this string (arrowhead) was selected for EM analysis (*C*) and reconstruction in 3D (*D*). (*E*) Most varicosities included one mitochondrion, which rarely filled the varicosity (as in *E*, *2*), but more readily occupied one-quarter to one-third of the volume (*E*, *1*). (*F*) Mitochondria occupied 28 ± 3% (mean ± SEM) of the varicosity on average ($n = 10$). (*G*) Immunogold labeling of NGPα RGL stem cell processes (scp, blue) from the GCL–ML border (granule neuron cell bodies, cb1–cb3, dark green; nuclei in black) apposed to the side of a granule neuron dendrite (gnd, light green). Serial sections of image in *G* are reconstructed in 3D and shown from both sides (*H* and *I*; Movie S6). Mitochondria-containing (m, black) varicosities extend processes, which wrap local axons (a1 and a2, red; *J* and *K*) or approach the synapses (arrowhead) formed by local axons (a3 and a4, red) with the granule neuron dendrite (*J–M*). (Scale bars: *A*, 20 μm; *B*, 10 μm; *C–E*, 0.5 μm; *E*, *1*, and *E*, *2*, 0.2 μm; *G–M*, 1 μm.)

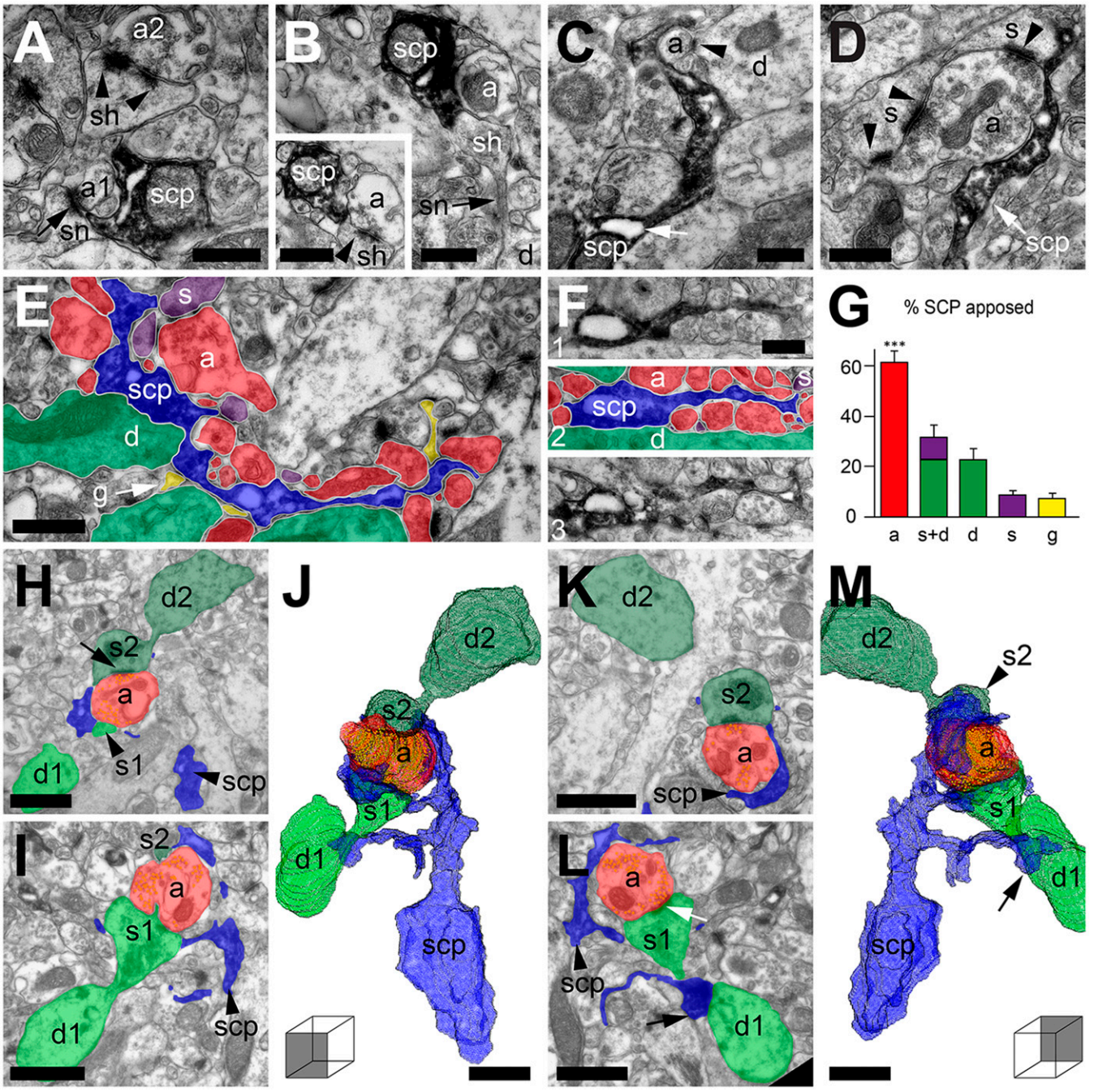

Fig. 5. RGL stem cell processes wrap local axons and synapses. (*A*) A DAB-labeled NGPα RGL stem cell process (scp) varicosity wrapping an axon (a1) forming an asymmetrical synapse (arrow) with a dendritic spine neck (sn). Arrowheads point to a second synapse made with the head of the same spine (sh). (*B*) An NGPα RGL stem cell varicosity directly apposing a spine head, extending from dendrite (d). (*Inset*) Adjacent section showing asymmetrical synapse (arrowhead). (*C*) A process from an NGPα RGL stem cell varicosity, wrapping an axon (a) and an asymmetrical synapse (arrowhead). Note also the reticulum-like inclusion (arrow) seen in the varicosity. (*D*) An NGPα RGL stem cell process wrapping a large axon terminal that forms asymmetrical synapses (arrowheads) with two dendritic spines (s). (*E*) An NGPα RGL stem cell process and the structures it apposes: axons (a), dendritic shafts (d), dendritic spines (s), and glia (g). (*F*) As for *E*, but the stem cell process (blue) apposes mainly axons (red) in its local vicinity. The adjacent serial sections (*1* and *3*) are shown without color overlays for comparison. (*G*) Proportion of varicosity membrane apposed by different structures [mean ± SEM of 10 varicosities, from four cells of three animals, 150 serial sections in total; one-way ANOVA with post hoc Dunnett test; $F_{(4,49)} = 31.38$, $P < 0.001$]. (*H–M*) Three-dimensional reconstruction (*J* and *M*; viewed from two angles; Movie S7) from serial EM frames, samples of which can be seen in *H*, *I*, *K*, and *L*. An NGPα RGL stem cell process (blue) wraps an inner ML axon terminal (red; vesicles in yellow), which forms asymmetrical synapses (arrows in *H* and *L*). (Scale bars: 0.5 μm.)

apposing synapses (Fig. 5 *A* and *B*). Varicosity surfaces therefore took on a concave form, as they arched around the mainly convex structures of small axon terminals and dendritic spines. Second, processes of varying lengths extended from the varicosities toward local asymmetrical synapses in a similar fashion to astrocytic processes (Fig. 5 *C* and *D*). Sometimes the association with the synapse was only one of apposing the edge of the synaptic cleft, but, other times, the process wrapped around the

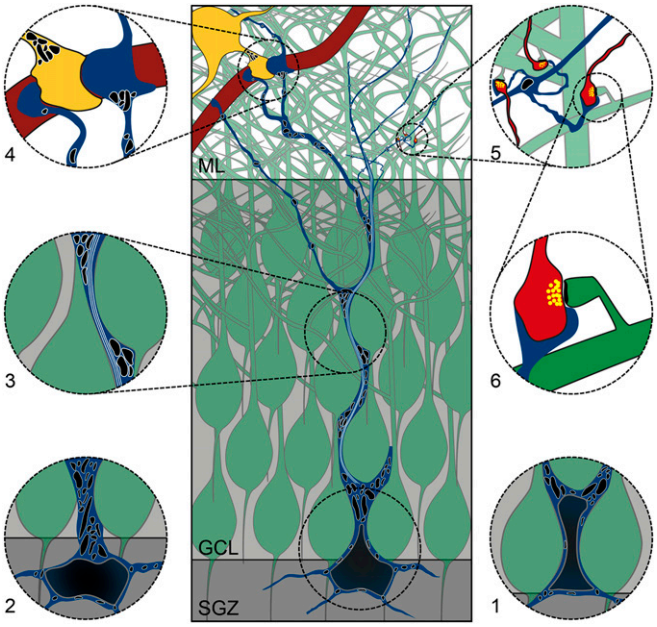

Fig. 6. RGL stem cell interactions with neuronal, vascular, and glial cells. The soma of the NGPα RGL stem cell (blue) sits above (*1*), across (*Center*), or below (*2*) the border of the SGZ and GCL, and takes different shapes. The primary process of the stem cell extends through the GCL (*3*), with its path and surface impacted on by granule neurons (green). Mitochondria (black) reside in the thicker parts of the process, but, in thinner regions, there is space only for the filaments (white) to grow through the process (*3*). Some processes in the ML make small endfeet-like contacts onto blood vessels (dark red) or wrap large thin sheets around them, sometimes continuing beyond the vessel after wrapping it (*4*). Astrocytic processes (yellow) share the blood vessel surface with the processes of the stem cell, with adhesion points where they meet. Thin processes possess regularly spaced mitochondria-filled varicosities along their length (*5*). Finer processes extend from these varicosities to approach and/or wrap around local asymmetrical synapses (light red; *5* and *6*).

whole axon terminal (Fig. 5*C*) and occasionally also the postsynaptic structure (Fig. 5*D*). The varicosities and their processes contained reticulum-like compartments into which the dark label could not penetrate. These were seen sitting next to mitochondria, in the varicosities themselves (Fig. 5 *A–C*, *E*, and *F*), or contained within the processes that extended from the varicosities (Fig. 5 *C–F*). It could be that these structures perform an important role related to the anatomical relationship of the stem cell processes with asymmetrical synapses.

Looking at individual EM frames of NGPα RGL stem cell varicosities, it was noticeable that the majority of their membranes were apposing neighboring axons. To quantify this relationship, we selected 10 varicosities at random (from four cells of three animals) and, across 150 serial sections, we measured the proportions of their membranes that were apposed by different structures. These structures included unmyelinated axons, dendritic shafts, dendritic spines, and glial processes. The varicosities more frequently apposed unmyelinated axons than any other individual structure [one-way ANOVA with a post hoc Dunnett test; $F_{(4,49)} = 31.38$, $P < 0.001$; Fig. 5*G*]. Seven of the 10 varicosities were analyzed further to establish their precise relationship with asymmetrical synapses of the ML. On average, these varicosities directly apposed the synaptic cleft of three asymmetrical synapses ($n = 7$; mean = 3.29 ± 0.35, SEM) and were within 0.5 μm of 13 asymmetrical synapses in 3D ($n = 7$; mean = 12.89 ± 1.43, SEM). Given that a typical NGPα RGL stem cell process arbor (Fig. 4 *A* and *B*) can possess 130 varicosities, this could suggest that its fine processes could appose ∼428 asymmetrical synapses in the inner ML and be within 0.5 μm of nearly four times as many ($n = 1,676$).

Many of the axons forming asymmetrical synapses in the inner third of the ML will be projections arriving from commissural fibers, hilar mossy cells, or the supramamillary nucleus (43), and the vast majority of postsynaptic structures will be the spines of granule cell dendrites. To demonstrate how tight the relationship of the NGPα RGL stem cell processes and these synapses could be, we traced an NGPα RGL stem cell process wrapping a large synapse-forming axon terminal in serial EM frames and reconstructed it in 3D (Fig. 5 *H–M* and Movie S7). The axon terminal formed asymmetrical synapses with the large mushroom spines of two dendrites (Fig. 5 *H* and *L*), and the stem cell process apposed both sides of each synapse, as well as the neck of one spine (Fig. 5 *L* and *M*). This tight association with local axons and synapses resembled the appositions seen for astrocytic processes (44), demonstrating yet another key feature of astrocytes mirrored by the processes of the NGPα RGL stem cell.

Discussion

The NGPα RGL stem cells of the mouse dentate gyrus have a highly complex and specialized morphology, with fine processes capable of invading all regions of the neurogenic niche, namely the GCL, the inner ML, the SGZ, and the hilus. In this study, we used Nestin-GFP transgenic mice and immunolabeling to identify NGPα RGL stem cells, and EM (TEM and SBF-SEM) to reveal the ultrastructure of their processes in 3D. Although no synaptic contacts were seen to be made with NGPα RGL stem cells, they were seen to directly appose asymmetrical synapses, blood vessels, granule neurons, astrocytes, and other NGPα RGL stem cells (Fig. 6). These structural interactions provide the anatomical framework for many of the factors identified as modulators of adult neurogenesis in the hippocampus.

Recent work has started to reveal heterogeneity within the population of dentate gyrus stem cells (22, 24, 28, 29). Stem cells with a horizontal morphology respond to various stimuli differently than those with a radial morphology (i.e., RGL stem cells) (22). RGL stem cells identified with different reporter mice (Nestin-GFP or GLAST-GFP) can play different roles in adult neurogenesis over different time scales (28). Even different Nestin-GFP mouse lines can label subtly different populations of Nestin-GFP–positive RGL stem cells (45–47). Using the same Nestin-reporter mouse as the present study, a previous study was able to characterize, by morphology, molecular marker expression, and clonal analysis, a Nestin-GFP–positive RGL stem cell that was able to proliferate and give rise to astrocytes, neurons, and other RGL cells: the type α Nestin-GFP–positive RGL stem cell (NGPα RGL stem cell) (29). By examining only Nestin-GFP–positive RGL stem cells with an NGPα RGL stem cell morphology, the present study focused on the proliferative population of Nestin-positive RGL stem cells. Further work will be required to assess whether the ultrastructural properties observed for NGPα RGL stem cells can be generalized to other dentate gyrus stem cells, such as (*i*) other Nestin-GFP–positive stem cells with different morphologies and fates, e.g., non-proliferative, NGPβ RGL stem cells (29) or stem cells with horizontal morphology (22), (*ii*) Nestin-GFP–positive RGL stem cells identified with different Nestin-GFP transgenic mouse lines (25, 45–47), (*iii*) RGL stem cells that are not Nestin-positive, approximately 30% of the total population (24) or those identified using other reporter mice (28), or (*iv*) RGL stem cells in the ventral hippocampus (48).

NGPα RGL Stem Cell Processes Define the Neurogenic Niche. Under the light microscope, the cell bodies of NGPα RGL stem cells appear distinct from those of their neighboring granule neurons and exhibit a variety of morphologies. When viewed in serial EM sections and reconstructed in 3D, NGPα RGL stem cell bodies

appear spheroid-, pyramidal-, or hourglass-shaped depending on whether they are in the SGZ, spanning the SGZ–GCL border, or entirely in the GCL, respectively (Fig. 6) (17, 19, 20). Their various morphologies are in sharp contrast to the relatively uniform morphologies of adjacent granule neuron cell bodies, whose tightly tessellated arrangement appears to impinge upon the more flexible shape of the stem cell. The imprints of granule neuron cell bodies also appear to contribute to the concave nature of the stem cell surfaces and the ridges present between them. Similar concave surfaces and ridges are seen for the primary process of the stem cell as it twists, turns, and curves around granule neuron cell bodies and primary dendrites en route to the ML (Fig. 6).

Similar morphological variety is seen in the contours of RGL stem cells in the tightly packed neurogenic niche of the SVZ (49), but this is not the case for embryonic cortical stem cells, which extend straight processes from smooth spheroid cell bodies, without the tight constraints of high cell body density (30). In the developing dentate gyrus, the first irregular contours of RGL stem cells appear at around postnatal day 3, when their radial processes begin to project across the more tightly packed GCL to the ML (50, 51). In the adult dentate gyrus, the NGPα RGL stem cell population is renewing (24, 29), and hence new primary processes are constantly extending through the GCL. The morphologies seen in the present study suggest that the flexible cytoskeleton of the NGPα RGL stem cell is exquisitely adapted to course its way through the more established architecture of the GCL.

At the edge of the ML, larger secondary and tertiary processes extend toward local blood vessels, wrapping them in large thin sheets, forming a patchwork coverage of the blood vessel surface alongside the processes of astrocytes (Fig. 6). Thin processes, with regular varicosities, extend finer processes toward local asymmetrical (i.e., putatively excitatory) synapses, approaching the synaptic cleft and/or ensheathing the synapse. The repeated nature of these process interactions with the surrounding vascular, glial, and neuronal environment is highly suggestive of underlying functions. As the vast majority of the NGPα RGL stem cell membrane comprises these processes, it could be argued that the neurogenic niche of the dentate gyrus is less rooted in the SGZ and more so in the inner third of the ML.

Synapse Wrapping by NGPα RGL Stem Cell Processes. In the present study, NGPα RGL stem cell processes in the ML are seen to approach and/or wrap asymmetrical synapses in a similar fashion to local astrocytes. This raises two key questions: (*i*) What function are NGPα RGL stem cell processes performing at the synapse? (*ii*) For which synapses are they performing this function?

Given their glia-like morphology, perisynaptic NGPα RGL stem cell processes could be acting as astrocytes. Astrocytes at the synapse take up excess glutamate, and are thought to release a host of factors, including neurotransmitters such as glutamate, ATP, and D-serine (52–55). These factors have the ability to regulate synaptic plasticity and contribute to the stability of synaptic connections, most notably those that are newly formed (56). If NGPα RGL stem cells could perform the same function in the inner third of the ML, they could promote the network integration of their own progeny by stabilizing their nascent synapses.

Alternatively, the function of perisynaptic NGPα RGL stem cell processes might be to gauge local network activity to regulate levels of neurogenesis. Single-cell RNA sequencing as well as subsequent electrophysiological analyses have recently shown that NGP RGL stem cells express functional glutamate receptors (ref. 57; but see also ref. 58 for contrast and ref. 59 for review). If these receptors are positioned perisynaptically, they might be able to detect fluctuations in local network activity via the amount of glutamate escaping from the synapse. A lower local network activity could result in less glutamate spillover and the activation of fewer glutamatergic receptors on the stem cell, and thus signal a greater need for new neurons. This could explain why blocking NMDA receptors in the dentate gyrus increases levels of adult neurogenesis in the dentate gyrus (60, 61, reviewed in ref. 62) and increases the numbers of RGL stem cells (63). Future experiments using immuno-EM approaches may help to identify and localize components crucial to these effects, such as glutamate receptors or transporters, in RGL stem cells.

NGPα RGL stem cell processes were seen to touch and/or ensheathe asymmetrical (putatively glutamatergic) synapses. Postsynaptic structures were identified as the dendritic spines of granule neurons, traced from the GCL, but the origin of presynaptic axons is less clear. The majority of glutamatergic inputs to the dentate gyrus originate from the entorhinal cortex (43), but cortical inputs mainly terminate in the outer two thirds of the ML (64–68). The dense arborizations of NGPα RGL stem cells are predominantly contained within the inner third of the ML and GCL, a region where subcortical inputs predominantly terminate (69). This might suggest that any glutamatergic signals received by stem cell processes would reflect the activity of subcortical inputs, such as long-range axons from the supramamillary nucleus (70). Notably, long-range serotonergic axons from the raphe arborize in the SVZ neurogenic niche and regulate the birth of new neurons (71). Other inputs to the inner ML emanate from commissural fibers or hilar mossy cells (72–74), which provide the first glutamatergic synapses onto newborn neurons of the dentate gyrus (75). Cell-specific stimulation of these neurons may help determine their action on the regulation of adult neuronal stem cells.

NGPα RGL Stem Cell Processes Within the Neurovascular Niche. In addition to the astrocyte-like wrapping of synapses, NGPα RGL stem cell processes also ensheathe blood vessels in an astrocyte-like manner (36). Thick processes branch toward local blood vessels, spreading across their surface, maximizing the surface area of the vessel they contact. This could suggest that signals released from the blood are attracting the stem cell process, stem cell process signals are attracting the blood vessel, or a mutual relationship exists whereby factors released from the blood and stem cell process benefit each other.

This relationship was first discussed in relation to whether a mitogenic signal, such as VEGF, was passed between the two structures to coregulate angiogenesis and neurogenesis (76). Although there are a collection of factors capable of influencing angiogenesis and neurogenesis, there are only a few neurogenic factors that are released from endothelial cells (77, 78). In addition, blood circulating factors have substantial effects over the process of neurogenesis (79–82). VEGF is one of these factors (83), and can stimulate neurogenesis (84–86) and reversibly modulate neuronal plasticity (87). Other blood-derived factors capable of affecting neurogenesis are glucocorticoids, which are necessary for the regulation of neuronal differentiation and migration (88). Adult neuronal stem cells themselves were recently shown to release a substantial VEGF-A signal (89), a signal that is received by other neuronal stem cells, via the VEGF receptor (VEGFR)2, and is necessary for maintenance of the RGL stem cell population. Additionally, a related VEGF ligand and receptor combination, VEGF-C and VEGFR3, respectively (90), was recently shown to directly control RGL stem cell activation in the hippocampus without effecting other cell types (91). Here, fine NGPα RGL stem cell processes were seen to appose the fine processes of neighboring stem cells, supporting the view that the autocrine secretion of proneurogenic factors may enable the autonomous regulation of stem cell activity.

As RGL stem cells secrete VEGF and their processes are comprehensively wrapping local blood vessels, it might be assumed that RGL stem cells are exerting a substantial control over angiogenesis and may participate in the formation of the

blood–brain barrier (BBB) on the newly formed blood vessels. Studies of physical exercise have shown that increases in neurogenesis with running (92) are coupled to increases in angiogenesis (93), and these factors are associated with an increase in cognitive function (94). Angiogenesis occurs alongside neurogenesis in embryonic development when the BBB is formed, but the BBB does not fully mature until 3 weeks postnatally, when cues from the neuroepithelium are thought to drive the wrapping of vessels by astrocytes (95). This gives plenty of opportunity to RGL stem cells in the developing dentate gyrus (50, 51) to receive similar cues and participate in the BBB via the wrapping of blood vessels. Furthermore, exogenous VEGF has been shown to increase the permeability of the BBB (96, 97). So the endogenous release of VEGF from perivascular RGL stem cell processes could participate in the induction of vasculogenesis and facilitate an increase in blood-to-brain signaling.

Blood vessels might also act as a site for the interaction between RGL stem cells and astrocytes. Here, we found that, where the two types of process met on the surface of the blood vessel, their membranes were of complementary thicknesses, and adhesion points existed between them. Astrocyte-expressed factors, such as Wnt3a, interleukins IL-1β and IL6, and ATP, promote differentiation of neural stem progenitor cells, whereas growth factor binding protein IGFBP6 and proteoglycan decorin inhibit their differentiation (98–100). Astrocyte–stem cell interactions have also been shown to regulate neurogenesis by secretion of ephrin-B2, which activates EphB4 receptors on the stem cell (101). Similar to the SVZ, where direct cell–cell contact between astrocytes and precursors stimulates neurogenesis (102), the extensive interaction between astrocytes and stem cell processes at the blood vessel surface in the dentate gyrus offers a stable structural platform through which astrocytic regulation of RGL stem cells could occur.

Conclusions

In this study, we have used a variety of LM and EM techniques to provide a detailed ultrastructural analysis of Nestin-GFP–positive adult RGL stem cells. The intimate relationship of their fine processes with synapses, blood vessels, and astrocytes provides a structural link between the local niche and the process of hippocampal neurogenesis. It supports the idea that the neurogenic niche plays an important role in the regulation of RGL stem cells, and that the niche itself could be considered to extend, with the processes of RGL stem cells, into the inner ML. Although the resolution of EM was required to reveal the fine elements observed here, further studies will be necessary to assess the function of the perisynaptic and perivascular structures described. By describing the fine structure of RGL stem cells, and their relationships with elements of the dentate gyrus neurogenic niche, we provide a necessary structural framework linking adult neural stem cells and the signals that activate and modulate their activity, and a new perspective on the process of adult neurogenesis.

Materials and Methods

Animal Handling. This study was carried out in strict accordance with the recommendations in the Guidance for the Care and Use of Laboratory Animals of the National Institutes of Health and was approved by the Swiss animal experimentation authorities. Every effort was made to minimize the number of animals used and their suffering. Nestin-GFP mice [male, P83-88; gift from the laboratory of K. Mori, Precursory Research for Embryonic Science and Technology (PRESTO), Japan Science and Technology Corporation, Soraku-gun, Kyoto] (37) were anesthetized, transcardially perfused with PBS solution (5 mL over 1 min) and then fixative [50 mL over 10 min, 4% paraformaldehyde (wt/vol); 0.1% glutaraldehyde (vol/vol) in 0.1 M phosphate buffer; (PB); Sigma], and kept at 4 °C for 24 h. Immunohistochemistry details are provided in *SI Materials and Methods*.

EM. Tissue was prepared as described in *SI Materials and Methods*. For TEM, seven NGPα RGL stem cells from Nestin-GFP transgenic mice were analyzed (four cells from three animals for DAB-peroxidase labeling and three cells from three animals for immunogold labeling), selected from 45 candidates identified at the LM level (29 DAB-peroxidase–labeled from three animals, 16 immunogold-labeled from three animals). For each of the seven cells, a mean of 10 regions of interest (ROIs; including cell bodies, primary processes, and blood vessel-wrapping or synapse-wrapping processes) were examined (±2 ROIs, SEM; 69 ROIs in total) in a mean of 29 serial sections each (±7 sections, SEM; 1,985 sections in total). For SBF-SEM, three RGL stem cells from three Nestin-GFP mice were microdissected from the tissue and processed.

ACKNOWLEDGMENTS. We thank Hongjun Song for comments on the manuscript and the Electron Microscope Facility and the Cellular Imaging Facility of the University of Lausanne. The SBF-SEM imaging performed at the University of California, San Diego, was supported by National Institutes of Health Grant GM103412 for the National Center for Microscopy and Imaging Research (to M.H.E.). J.M. and N.T. were funded by the IBRO-SSN Fellowship for Young Investigators, Fondation Leenaards, and the Swiss National Science Foundation. I.S-P. and R.O. were participants in the Summer Undergraduate Research Programme of the University of Lausanne.

1. Altman J, Das GD (1965) Autoradiographic and histological evidence of postnatal hippocampal neurogenesis in rats. *J Comp Neurol* 124(3):319–335.
2. Gould E (2007) How widespread is adult neurogenesis in mammals? *Nat Rev Neurosci* 8(6):481–488.
3. Ming GL, Song H (2011) Adult neurogenesis in the mammalian brain: Significant answers and significant questions. *Neuron* 70(4):687–702.
4. Kriegstein A, Alvarez-Buylla A (2009) The glial nature of embryonic and adult neural stem cells. *Annu Rev Neurosci* 32:149–184.
5. Bonaguidi MA, Song J, Ming GL, Song H (2012) A unifying hypothesis on mammalian neural stem cell properties in the adult hippocampus. *Curr Opin Neurobiol* 22(5): 754–761.
6. Toni N, Sultan S (2011) Synapse formation on adult-born hippocampal neurons. *Eur J Neurosci* 33(6):1062–1068.
7. Lee SW, Clemenson GD, Gage FH (2012) New neurons in an aged brain. *Behav Brain Res* 227(2):497–507.
8. Vivar C, van Praag H (2013) Functional circuits of new neurons in the dentate gyrus. *Front Neural Circuits* 7:15.
9. Braun SM, Jessberger S (2014) Adult neurogenesis: Mechanisms and functional significance. *Development* 141(10):1983–1986.
10. Deng W, Aimone JB, Gage FH (2010) New neurons and new memories: How does adult hippocampal neurogenesis affect learning and memory? *Nat Rev Neurosci* 11(5):339–350.
11. Marín-Burgin A, Schinder AF (2012) Requirement of adult-born neurons for hippocampus-dependent learning. *Behav Brain Res* 227(2):391–399.
12. O'Leary OF, Cryan JF (2014) A ventral view on antidepressant action: Roles for adult hippocampal neurogenesis along the dorsoventral axis. *Trends Pharmacol Sci* 35(12): 675–687.
13. Doetsch F, Caillé I, Lim DA, García-Verdugo JM, Alvarez-Buylla A (1999) Subventricular zone astrocytes are neural stem cells in the adult mammalian brain. *Cell* 97(6):703–716.
14. Mirzadeh Z, Merkle FT, Soriano-Navarro M, Garcia-Verdugo JM, Alvarez-Buylla A (2008) Neural stem cells confer unique pinwheel architecture to the ventricular surface in neurogenic regions of the adult brain. *Cell Stem Cell* 3(3):265–278.
15. Beckervordersandforth R, et al. (2010) In vivo fate mapping and expression analysis reveals molecular hallmarks of prospectively isolated adult neural stem cells. *Cell Stem Cell* 7(6):744–758.
16. Morrens J, Van Den Broeck W, Kempermann G (2012) Glial cells in adult neurogenesis. *Glia* 60(2):159–174.
17. Kosaka T, Hama K (1986) Three-dimensional structure of astrocytes in the rat dentate gyrus. *J Comp Neurol* 249(2):242–260.
18. Seri B, García-Verdugo JM, McEwen BS, Alvarez-Buylla A (2001) Astrocytes give rise to new neurons in the adult mammalian hippocampus. *J Neurosci* 21(18):7153–7160.
19. Seki T (2003) Microenvironmental elements supporting adult hippocampal neurogenesis. *Anat Sci Int* 78(2):69–78.
20. Seri B, García-Verdugo JM, Collado-Morente L, McEwen BS, Alvarez-Buylla A (2004) Cell types, lineage, and architecture of the germinal zone in the adult dentate gyrus. *J Comp Neurol* 478(4):359–378.
21. Seki T, Namba T, Mochizuki H, Onodera M (2007) Clustering, migration, and neurite formation of neural precursor cells in the adult rat hippocampus. *J Comp Neurol* 502(2):275–290.
22. Lugert S, et al. (2010) Quiescent and active hippocampal neural stem cells with distinct morphologies respond selectively to physiological and pathological stimuli and aging. *Cell Stem Cell* 6(5):445–456.
23. Namba T, et al. (2005) The fate of neural progenitor cells expressing astrocytic and radial glial markers in the postnatal rat dentate gyrus. *Eur J Neurosci* 22(8): 1928–1941.
24. Bonaguidi MA, et al. (2011) In vivo clonal analysis reveals self-renewing and multipotent adult neural stem cell characteristics. *Cell* 145(7):1142–1155.
25. Dranovsky A, et al. (2011) Experience dictates stem cell fate in the adult hippocampus. *Neuron* 70(5):908–923.

26. Encinas JM, et al. (2011) Division-coupled astrocytic differentiation and age-related depletion of neural stem cells in the adult hippocampus. *Cell Stem Cell* 8(5):566–579.
27. Kempermann G (2011) The pessimist's and optimist's views of adult neurogenesis. *Cell* 145(7):1009–1011.
28. DeCarolis NA, et al. (2013) In vivo contribution of nestin- and GLAST-lineage cells to adult hippocampal neurogenesis. *Hippocampus* 23(8):708–719.
29. Gebara E, et al. (2016) Heterogeneity of radial glia-like cells in the adult hippocampus. *Stem Cells*, 10.1002/stem.2266.
30. Noctor SC, Flint AC, Weissman TA, Dammerman RS, Kriegstein AR (2001) Neurons derived from radial glial cells establish radial units in neocortex. *Nature* 409(6821): 714–720.
31. Sun GJ, et al. (2015) Tangential migration of neuronal precursors of glutamatergic neurons in the adult mammalian brain. *Proc Natl Acad Sci USA* 112(30):9484–9489.
32. Shihabuddin LS, Horner PJ, Ray J, Gage FH (2000) Adult spinal cord stem cells generate neurons after transplantation in the adult dentate gyrus. *J Neurosci* 20(23): 8727–8735.
33. Song H, Stevens CF, Gage FH (2002) Astroglia induce neurogenesis from adult neural stem cells. *Nature* 417(6884):39–44.
34. Anthony TE, Klein C, Fishell G, Heintz N (2004) Radial glia serve as neuronal progenitors in all regions of the central nervous system. *Neuron* 41(6):881–890.
35. Silva-Vargas V, Crouch EE, Doetsch F (2013) Adult neural stem cells and their niche: A dynamic duo during homeostasis, regeneration, and aging. *Curr Opin Neurobiol* 23(6):935–942.
36. Filippov V, et al. (2003) Subpopulation of nestin-expressing progenitor cells in the adult murine hippocampus shows electrophysiological and morphological characteristics of astrocytes. *Mol Cell Neurosci* 23(3):373–382.
37. Yamaguchi M, Saito H, Suzuki M, Mori K (2000) Visualization of neurogenesis in the central nervous system using nestin promoter-GFP transgenic mice. *Neuroreport* 11(9):1991–1996.
38. Shapiro LA, Korn MJ, Shan Z, Ribak CE (2005) GFAP-expressing radial glia-like cell bodies are involved in a one-to-one relationship with doublecortin-immunolabeled newborn neurons in the adult dentate gyrus. *Brain Res* 1040(1-2):81–91.
39. Denk W, Horstmann H (2004) Serial block-face scanning electron microscopy to reconstruct three-dimensional tissue nanostructure. *PLoS Biol* 2(11):e329.
40. Peters A, Palay SL, Webster HdeF (1970) *The Fine Structure of the Nervous System* (Oxford Univ Press, Oxford, UK).
41. Hama K, Arii T, Katayama E, Marton M, Ellisman MH (2004) Tri-dimensional morphometric analysis of astrocytic processes with high voltage electron microscopy of thick Golgi preparations. *J Neurocytol* 33(3):277–285.
42. Mathiisen TM, Lehre KP, Danbolt NC, Ottersen OP (2010) The perivascular astroglial sheath provides a complete covering of the brain microvessels: An electron microscopic 3D reconstruction. *Glia* 58(9):1094–1103.
43. Leranth C, Hajszan T (2007) Extrinsic afferent systems to the dentate gyrus. *Prog Brain Res* 163:63–84.
44. Witcher MR, Kirov SA, Harris KM (2007) Plasticity of perisynapticastroglia during synaptogenesis in the mature rat hippocampus. *Glia* 55(1):13–23.
45. Encinas JM, Vaahtokari A, Enikolopov G (2006) Fluoxetine targets early progenitor cells in the adult brain. *Proc Natl Acad Sci USA* 103(21):8233–8238.
46. Balordi F, Fishell G (2007) Mosaic removal of hedgehog signaling in the adult SVZ reveals that the residual wild-type stem cells have a limited capacity for self-renewal. *J Neurosci* 27(52):14248–14259.
47. Lagace DC, et al. (2007) Dynamic contribution of nestin-expressing stem cells to adult neurogenesis. *J Neurosci* 27(46):12623–12629.
48. Jinno S (2011) Topographic differences in adult neurogenesis in the mouse hippocampus: A stereology-based study using endogenous markers. *Hippocampus* 21(5): 467–480.
49. Danilov AI, et al. (2009) Ultrastructural and antigenic properties of neural stem cells and their progeny in adult rat subventricular zone. *Glia* 57(2):136–152.
50. Brunne B, et al. (2010) Origin, maturation, and astroglial transformation of secondary radial glial cells in the developing dentate gyrus. *Glia* 58(13):1553–1569.
51. Nicola Z, Fabel K, Kempermann G (2015) Development of the adult neurogenic niche in the hippocampus of mice. *Front Neuroanat* 9:53.
52. Huang YH, Bergles DE (2004) Glutamate transporters bring competition to the synapse. *Curr Opin Neurobiol* 14(3):346–352.
53. Volterra A, Meldolesi J (2005) Astrocytes, from brain glue to communication elements: The revolution continues. *Nat Rev Neurosci* 6(8):626–640.
54. Bains JS, Oliet SH (2007) Glia: They make your memories stick! *Trends Neurosci* 30(8): 417–424.
55. Hamilton NB, Attwell D (2010) Do astrocytes really exocytose neurotransmitters? *Nat Rev Neurosci* 11(4):227–238.
56. Ota Y, Zanetti AT, Hallock RM (2013) The role of astrocytes in the regulation of synaptic plasticity and memory formation. *Neural Plast* 2013:185463.
57. Shin J, et al. (2015) Single-Cell RNA-seq with waterfall reveals molecular cascades underlying adult neurogenesis. *Cell Stem Cell* 17(3):360–372.
58. Tozuka Y, Fukuda S, Namba T, Seki T, Hisatsune T (2005) GABAergic excitation promotes neuronal differentiation in adult hippocampal progenitor cells. *Neuron* 47(6):803–815.
59. Jansson LC, Åkerman KE (2014) The role of glutamate and its receptors in the proliferation, migration, differentiation and survival of neural progenitor cells. *J Neural Transm (Vienna)* 121(8):819–836.
60. Cameron HA, McEwen BS, Gould E (1995) Regulation of adult neurogenesis by excitatory input and NMDA receptor activation in the dentate gyrus. *J Neurosci* 15(6): 4687–4692.
61. Nacher J, Rosell DR, Alonso-Llosa G, McEwen BS (2001) NMDA receptor antagonist treatment induces a long-lasting increase in the number of proliferating cells, PSA-NCAM-immunoreactive granule neurons and radial glia in the adult rat dentate gyrus. *Eur J Neurosci* 13(3):512–520.
62. Taylor CJ, He R, Bartlett PF (2014) The role of the N-methyl-D-aspartate receptor in the proliferation of adult hippocampal neural stem and precursor cells. *Sci China Life Sci* 57(4):403–411.
63. Namba T, Maekawa M, Yuasa S, Kohsaka S, Uchino S (2009) The Alzheimer's disease drug memantine increases the number of radial glia-like progenitor cells in adult hippocampus. *Glia* 57(10):1082–1090.
64. Bellocchio EE, et al. (1998) The localization of the brain-specific inorganic phosphate transporter suggests a specific presynaptic role in glutamatergic transmission. *J Neurosci* 18(21):8648–8659.
65. Fremeau RT, Jr, et al. (2001) The expression of vesicular glutamate transporters defines two classes of excitatory synapse. *Neuron* 31(2):247–260.
66. Fremeau RT, Jr, Voglmaier S, Seal RP, Edwards RH (2004) VGLUTs define subsets of excitatory neurons and suggest novel roles for glutamate. *Trends Neurosci* 27(2): 98–103.
67. Kaneko T, Fujiyama F (2002) Complementary distribution of vesicular glutamate transporters in the central nervous system. *Neurosci Res* 42(4):243–250.
68. Kaneko T, Fujiyama F, Hioki H (2002) Immunohistochemical localization of candidates for vesicular glutamate transporters in the rat brain. *J Comp Neurol* 444(1): 39–62.
69. Halasy K, Hajszan T, Kovács EG, Lam TT, Leranth C (2004) Distribution and origin of vesicular glutamate transporter 2-immunoreactive fibers in the rat hippocampus. *Hippocampus* 14(7):908–918.
70. Soussi R, Zhang N, Tahtakran S, Houser CR, Esclapez M (2010) Heterogeneity of the supramammillary-hippocampal pathways: Evidence for a unique GABAergic neurotransmitter phenotype and regional differences. *Eur J Neurosci* 32(5):771–785.
71. Tong CK, et al. (2014) Axonal control of the adult neural stem cell niche. *Cell Stem Cell* 14(4):500–511.
72. Amaral DG, Scharfman HE, Lavenex P (2007) The dentate gyrus: Fundamental neuroanatomical organization (dentate gyrus for dummies). *Prog Brain Res* 163:3–22.
73. Buckmaster PS, Wenzel HJ, Kunkel DD, Schwartzkroin PA (1996) Axon arbors and synaptic connections of hippocampal mossy cells in the rat *in vivo*. *J Comp Neurol* 366(2):271–292.
74. Frotscher M, Seress L, Schwerdtfeger WK, Buhl E (1991) The mossy cells of the fascia dentata: A comparative study of their fine structure and synaptic connections in rodents and primates. *J Comp Neurol* 312(1):145–163.
75. Chancey JH, Poulsen DJ, Wadiche JI, Overstreet-Wadiche L (2014) Hilar mossy cells provide the first glutamatergic synapses to adult-born dentate granule cells. *J Neurosci* 34(6):2349–2354.
76. Palmer TD, Willhoite AR, Gage FH (2000) Vascular niche for adult hippocampal neurogenesis. *J Comp Neurol* 425(4):479–494.
77. Goldman SA, Chen Z (2011) Perivascular instruction of cell genesis and fate in the adult brain. *Nat Neurosci* 14(11):1382–1389.
78. Shen Q, et al. (2004) Endothelial cells stimulate self-renewal and expand neurogenesis of neural stem cells. *Science* 304(5675):1338–1340.
79. Villeda SA, et al. (2011) The ageing systemic milieu negatively regulates neurogenesis and cognitive function. *Nature* 477(7362):90–94.
80. Villeda SA, Wyss-Coray T (2013) The circulatory systemic environment as a modulator of neurogenesis and brain aging. *Autoimmun Rev* 12(6):674–677.
81. Villeda SA, et al. (2014) Young blood reverses age-related impairments in cognitive function and synaptic plasticity in mice. *Nat Med* 20(6):659–663.
82. Stolp HB, Molnár Z (2015) Neurogenic niches in the brain: Help and hindrance of the barrier systems. *Front Neurosci* 9:20.
83. Leung DW, Cachianes G, Kuang WJ, Goeddel DV, Ferrara N (1989) Vascular endothelial growth factor is a secreted angiogenic mitogen. *Science* 246(4935): 1306–1309.
84. Schänzer A, et al. (2004) Direct stimulation of adult neural stem cells in vitro and neurogenesis in vivo by vascular endothelial growth factor. *Brain Pathol* 14(3): 237–248.
85. Jin K, et al. (2002) Vascular endothelial growth factor (VEGF) stimulates neurogenesis in vitro and in vivo. *Proc Natl Acad Sci USA* 99(18):11946–11950.
86. Fournier NM, Lee B, Banasr M, Elsayed M, Duman RS (2012) Vascular endothelial growth factor regulates adult hippocampal cell proliferation through MEK/ERK- and PI3K/Akt-dependent signaling. *Neuropharmacology* 63(4):642–652.
87. Licht T, et al. (2011) Reversible modulations of neuronal plasticity by VEGF. *Proc Natl Acad Sci USA* 108(12):5081–5086.
88. Fitzsimons CP, et al. (2013) Knockdown of the glucocorticoid receptor alters functional integration of newborn neurons in the adult hippocampus and impairs fear-motivated behavior. *Mol Psychiatry* 18(9):993–1005.
89. Kirby ED, Kuwahara AA, Messer RL, Wyss-Coray T (2015) Adult hippocampal neural stem and progenitor cells regulate the neurogenic niche by secreting VEGF. *Proc Natl Acad Sci USA* 112(13):4128–4133.
90. Ferrara N, Gerber HP, LeCouter J (2003) The biology of VEGF and its receptors. *Nat Med* 9(6):669–676.
91. Han J, et al. (2015) Vascular endothelial growth factor receptor 3 controls neural stem cell activation in mice and humans. *Cell Reports* 10(7):1158–1172.
92. van Praag H, Kempermann G, Gage FH (1999) Running increases cell proliferation and neurogenesis in the adult mouse dentate gyrus. *Nat Neurosci* 2(3):266–270.
93. Van der Borght K, et al. (2009) Physical exercise leads to rapid adaptations in hippocampal vasculature: Temporal dynamics and relationship to cell proliferation and neurogenesis. *Hippocampus* 19(10):928–936.
94. Clark PJ, Brzezinska WJ, Puchalski EK, Krone DA, Rhodes JS (2009) Functional analysis of neurovascular adaptations to exercise in the dentate gyrus of young adult mice associated with cognitive gain. *Hippocampus* 19(10):937–950.

95. Tam SJ, Watts RJ (2010) Connecting vascular and nervous system development: Angiogenesis and the blood-brain barrier. *Annu Rev Neurosci* 33:379–408.
96. Keck PJ, et al. (1989) Vascular permeability factor, an endothelial cell mitogen related to PDGF. *Science* 246(4935):1309–1312.
97. Jiang S, Xia R, Jiang Y, Wang L, Gao F (2014) Vascular endothelial growth factors enhance the permeability of the mouse blood-brain barrier. *PLoS One* 9(2):e86407.
98. Lie DC, et al. (2005) Wnt signalling regulates adult hippocampal neurogenesis. *Nature* 437(7063):1370–1375.
99. Barkho BZ, et al. (2006) Identification of astrocyte-expressed factors that modulate neural stem/progenitor cell differentiation. *Stem Cells Dev* 15(3):407–421.
100. Cao X, et al. (2013) Astrocytic adenosine 5′-triphosphate release regulates the proliferation of neural stem cells in the adult hippocampus. *Stem Cells* 31(8):1633–1643.
101. Ashton RS, et al. (2012) Astrocytes regulate adult hippocampal neurogenesis through ephrin-B signaling. *Nat Neurosci* 15(10):1399–1406.
102. Lim DA, Alvarez-Buylla A (1999) Interaction between astrocytes and adult subventricular zone precursors stimulates neurogenesis. *Proc Natl Acad Sci USA* 96(13):7526–7531.
103. Gebara E, Sultan S, Kocher-Braissant J, Toni N (2013) Adult hippocampal neurogenesis inversely correlates with microglia in conditions of voluntary running and aging. *Front Neurosci* 7:145.
104. Wilke SA, et al. (2013) Deconstructing complexity: Serial block-face electron microscopic analysis of the hippocampal mossy fiber synapse. *J Neurosci* 33(2):507–522.
105. Kremer JR, Mastronarde DN, McIntosh JR (1996) Computer visualization of three-dimensional image data using IMOD. *J Struct Biol* 116(1):71–76.